2026 IEEE International Conference on Robotics and Automation (ICRA 2026)
June 1-5, 2026. Vienna, Austria

Quartic Oscillator Model with Applications in Locomotion

André S. Carvalho[1], Miguel A. Botto and Jorge M. Martins

***Abstract*— This work introduces a novel compliant model for running gaits. The model consists of a linear leg stiffness paired with a nonlinear energy regulation term. This new model, termed the quartic model, is shown to reproduce the external dynamics of a running gait. The characteristics of the gait are imposed through parametric conditions which are derived through linearization of the model. The nonlinear nature of the model ensures convergence towards a limit cycle, which makes the model a useful template for the control of legged systems.**

I. INTRODUCTION

The study of animal locomotion is central to the development of prosthetic, orthotic, and exoskeletal devices, with applications ranging from rehabilitation and assistance to the enhancement of human physical capabilities. A key challenge in this field lies in designing models that balance biological relevance with parameter transparency, ensuring that the reasoning behind parameter selection is explicit and representative of locomotion dynamics.

Oscillations play a fundamental role in locomotion, where elasticity emerges as a dominant mechanism, as best exemplified through the spring-mass model of locomotion [1]. In a rigid body framework, this can be captured either by prescribing external dynamics, using force [2] or impedance control [3] techniques, or through exploration of the dynamic interplay between elastic elements and the rigid body segments [4]. It is also relevant that such oscillations are self-sustained in the form of a limit cycle, allowing perturbations to be compensated in a way that allows the return to the original gait [5]. Alternatively, a method which is closely related to sustained oscillations relies on the use of central pattern generators (CPGs), where neural-inspired oscillators directly shape joint trajectories [6], [7].

From a biological perspective, muscle-tendon units mediate mechanical energy through a combination of storage, damping and generation. Here, the tendon is very efficient at storing energy (with at most 10% of energy loss [8]), while the velocity-dependent dynamics of muscle fibers allow for the regulation of energy during steady state or transient locomotion tasks. These principles have been abstracted into phenomenological muscle models, where energy regulation emerges through muscle fibers stimulation, either through length, velocity, or force reflex pathways [9]. Here, at a more abstract and simplified level, the quartic model echoes this bioinspired approach by expressing the energy regulation action at the velocity level. Thus, the present work builds upon the elastic spring-mass model, with its multitude of variations [10], and also on the construction of nonlinear oscillators which are representative of locomotion.

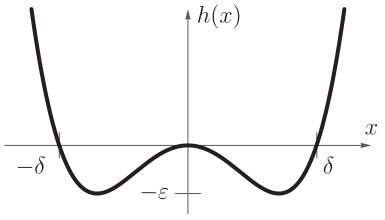

Fig. 1. Quartic energy function, $h(x) = \varepsilon\,(\frac{x^4}{\delta^2} - x^2)$.

To do so, the one-dimensional quartic oscillator is here presented (§II) by analogy with the well-known Van der Pol oscillator. In the previous context, this novel model pairs the elasticity of the spring-mass model with a quartic displacement function that, in proportion to velocity, achieves energy regulation. Inclusion of gravity terms (§III) and its discretization into stance and flight events (§IV) are also detailed. Approximate solutions are discussed throughout before defining the quartic running model, in two-dimensional space (§V). These approximations allow transparency in the tuning of the model, by predicting the characteristics of the resulting running gait. This feature is illustrated by modeling the gait characteristics of runners [11], using as inputs the desired velocity, the total mass, the leg's length and the flight and stance periods of time. Although a proof of stability for the two-dimensional case is not provided here, all one-dimensional variants are proved to be stable, as detailed in the Appendix.

II. QUARTIC OSCILLATOR

It is the goal of this section to define the quartic oscillator model, as well as provide some intuition for the existence of limit cycles for the model. Whenever possible, this matter is addressed more rigorously using the results in the Appendix. As a constructive example, consider first a well known system which exhibits periodic solutions, given here by the Van der Pol oscillator described by the autonomous system $\mathring{\mathring{x}} + \varepsilon\left(x^2 - \delta^2\right)\mathring{x} + x = 0$, with $\varepsilon > 0$ and $\delta > 0$. Here, the circle notation is introduced, in order to distinguish derivatives with respect to an independent coordinate, other than time. That is, $\mathring{x} = \frac{dx}{d\tau}$ and $\mathring{\mathring{x}} = \frac{d^2x}{d\tau^2}$. This model is comprised by a linear elasticity and a nonlinear damping. This system is a particular case of the Liénard equation [12], known by its general formulation

$$\mathring{\mathring{x}} + h(x)\,\mathring{x} + g(x) = 0\,. \tag{1}$$

[1]Corresponding author: André S. Carvalho,
andre.s.carvalho@tecnico.ulisboa.pt
All authors are with IDMEC, Instituto Superior Técnico, Universidade de Lisboa, Portugal, Av. Rovisco Pais, 1049-001 Lisboa.

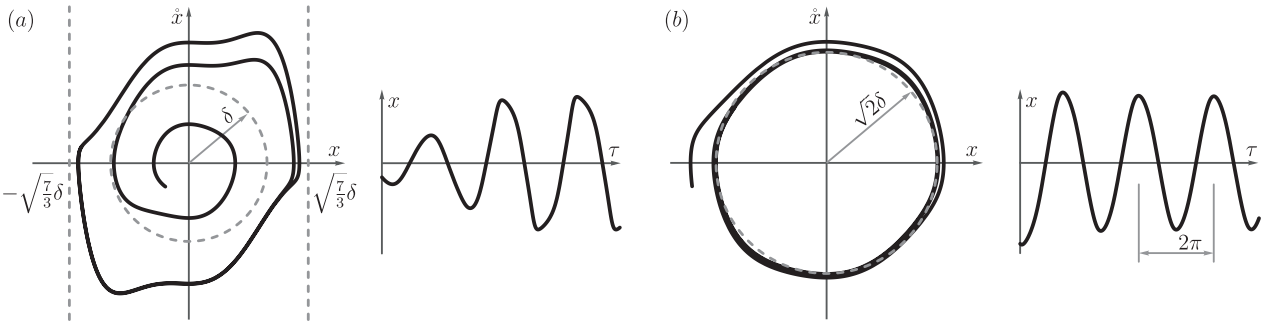

Fig. 2. Numerical solutions for the quartic oscillator (2) with (a) large energy coefficient, $\varepsilon = 3$, and (b) small energy coefficient, $\varepsilon = 0.5$.

Given this definition, some properties which promote the emergence of limit cycles in the Van der Pol oscillator can be inspected. In particular, it is pertinent to note that the nonlinear term, $h(x)\,\mathring{x}$, undergoes a sign change across its motion along x. That is, it is dissipative on the interval $|x| > \delta$ and generative in the interval $|x| < \delta$. This is also a good indication that the equilibrium, $(x, \mathring{x}) = \mathbf{0}$, must be unstable, and that all trajectories starting in the generative region are bound to escape it. Moreover, since this generative region is surrounded by another region of dissipative nature, this also indicates that the trajectories are not able to perpetually escape from the origin. These are strong indicators that the system is bound to converge towards a periodic solution. Such attractiveness towards a periodic solution is called a limit cycle.

To better motivate the definition of the quartic model, it is relevant to first see why the Van der Pol oscillator is not a good model for locomotion. That said, stance events are well described by the elastic element $g(x) = x$, in accordance to compliant models of locomotion [1]. Thus, a stance phase could be extracted from the Liénard equation (1), to write $\mathring{\mathring{x}} + h(x)\,\mathring{x} + x = 0$ for all $x \geq 0$. However, using the Van der Pol's dissipative function, the instant of touchdown would translate into a discontinuity in the leg's support force, $h(0)\,\mathring{x}(0) = -\varepsilon\,\delta^2\,\mathring{x}(0)$. To remove this discontinuity, a new nonlinear energy function is defined in such a way that $h(0) = 0$. Choosing a fourth order polynomial, a possible choice results in the following quartic model,

$$\mathring{\mathring{x}} + \varepsilon\left(\frac{x^4}{\delta^2} - x^2\right)\mathring{x} + x = 0\,, \quad \text{with} \quad \varepsilon > 0,\, \delta > 0\,. \tag{2}$$

This energy function is illustrated in Fig. 1. Again, much like the Van der Pol model, $h(x) = 0$ when $x = \pm\delta$, and all previous intuitive remarks for the existence of limit cycles are echoed here. Indeed, as shown in Corollary 1, the limit cycle exists and is unique. Moreover, the limit cycle's trajectory is bound from the inside by $x^2 + \mathring{x}^2 > \delta^2$, and bound from the outside by $|x| < \sqrt{\frac{7}{3}}\,\delta$. The state-space trajectories of the model are illustrated in Figs. 2(a,b). Fig. 2(b) is a special case, where energy regulation is very small. In such a case, the solution approaches a linear solution, with state-space amplitude $A = \sqrt{2}\,\delta$, and oscillation period of $\Delta\tau = 2\,\pi$. The linearized solution will prove to be quite useful, and is detailed in the following section.

III. ACCELERATED QUARTIC OSCILLATOR

With the goal of describing a stance event, it is useful here to imbue the oscillator with an acceleration bias, α, which will later be used to model gravity. That said, the accelerated quartic oscillator is described by

$$\mathring{\mathring{x}} + \varepsilon\left(\frac{x^4}{\delta^2} - x^2\right)\mathring{x} + x - \alpha = 0\,, \text{ with } \quad \varepsilon > 0,\, \delta > \alpha > 0\,. \tag{3}$$

Corollary 2 guarantees the existence of limit cycles for this system. This system will be useful in the estimation of stance parameters. Particularly, in its linearized form, which is obtained as follows.

To linearly approximate (3), consider employing an energy-balance method for the limit cycle [12]. To do so, assume a very small energetic coefficient, $|\varepsilon| \ll 1$, which in turn allows to state that the nonlinearity is negligible. In particular, when $\varepsilon = 0$, the system (3) becomes purely elastic, with some bias,

$$\mathring{\mathring{x}} + x - \alpha = 0\,, \tag{4}$$

which one may term as the linearized system. It is well known that the general solution is $x(\tau) = \alpha + A\,\cos(\tau + \phi)$, where A denotes the amplitude of oscillation and ϕ an angle offset, both due to initial conditions. Since the rate of change is $\mathring{x}(\tau) = -A\,\sin(\tau + \phi)$, one may further restrict the solutions for the case that $A > 0$ and $\phi = 0$, to write the phase paths of the linearized system as

$$x = \alpha + A\,\cos\tau\,, \quad \mathring{x} = -A\,\sin\tau\,, \tag{5}$$

with an oscillation period given by $T = 2\,\pi$. Now, defining a potential energy function for the nonlinear system (3), as $G(x) = \int_0^x g(u)\,du = \frac{1}{2}x^2 - \alpha\,x$, and the kinetic energy as $\mathcal{T}(\mathring{x}) = \frac{1}{2}\mathring{x}^2$. Then, the total energy becomes

$$\mathcal{E}(t) = \frac{1}{2}\mathring{x}^2(\tau) + \frac{1}{2}x^2(\tau) - \alpha\,x(\tau)\,, \tag{6}$$

and the total energy change over one period of oscillation of the limit cycle is

$$\mathcal{E}(T) - \mathcal{E}(0) = -\int_0^T h(x(\tau))\,\mathring{x}^2(\tau)\,d\tau = 0\,. \tag{7}$$

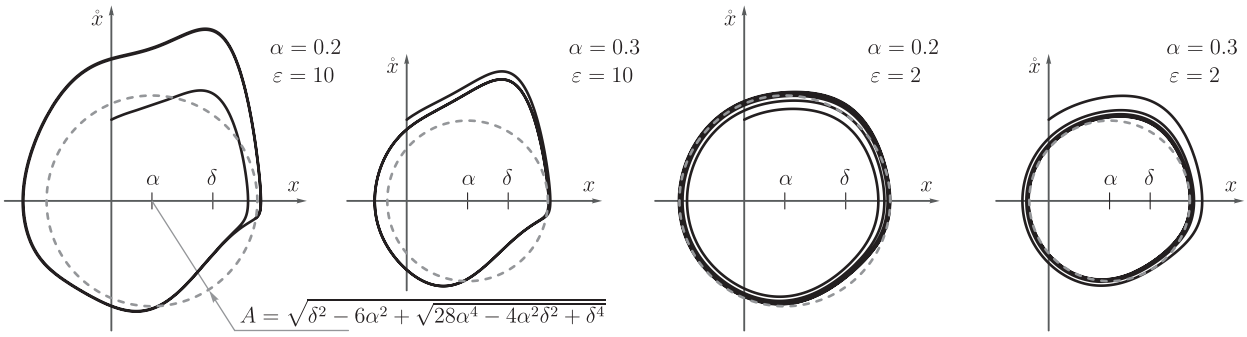

Fig. 3. Numerical solutions for the accelerated quartic oscillator (3) with $\delta = 0.5$.

Here, the fact that the limit cycle is a closed path means that the change in energy must be null. This energy variation is now approximated by introducing the phase paths of the linearized system (5), together with their oscillation period. Allowing to state from (7) that

$$\int_0^{2\pi} h(\alpha + A\,\cos\tau)\,\sin^2\tau\,d\tau = 0\,. \tag{8}$$

Solving this equation gives the amplitude of the accelerated quartic oscillator's linearized solution,

$$A = \sqrt{\delta^2 - 6\alpha^2 + \sqrt{28\alpha^4 - 4\alpha^2\delta^2 + \delta^4}}\,. \tag{9}$$

When $\alpha = 0$, the solution degenerates into the non-accelerated quartic model's approximated amplitude, with $A = \sqrt{2}\,\delta$, which was previously illustrated in Fig. 2(b). The solutions of the accelerated quartic oscillator are compared with their corresponding amplitude approximation in Fig. 3, with varying energy regulation, ε, and acceleration bias, α.

IV. HOPPING MODEL

The hopping model (or hop in place model) is now proposed, through hybridization [13] of the accelerated quartic oscillator (3). Before doing so, it seems now to be an opportune moment to imbue the model with some physical meaning. In particular, the focus is now placed in the introduction of mass, gravity, stiffness and time into the model. That said, let x [m] be a displacement and time be $t = \tau/\omega$ [s]. Then, (3) is given physical meaning through $m\,\ddot{x} + m\,\omega\,\varepsilon\left(x^4/\delta^2 - x^2\right)\dot{x} + m\,\omega^2\,(x-\alpha) = 0$. Here, m [kg] denotes mass, in which case $f = m\,\ddot{x}$ [N] represents a force. In particular, if $k = m\,\omega^2$ [N/m] denotes stiffness, it must be that $\omega = \sqrt{k/m}$ [s^{-1}]. And, if $m\,\omega^2\,\alpha = m\,\mathrm{g}$ denotes force due to gravity, it must be that $\alpha = \mathrm{g}/\omega^2$ [m]. Keeping the focus on the acceleration, then

$$\ddot{x} + \omega\,\varepsilon\left(\frac{x^4}{\delta^2} - x^2\right)\dot{x} + \omega^2\,(x-\alpha) = 0\,, \tag{10}$$

$$\text{with}\quad \delta > \alpha = \frac{\mathrm{g}}{\omega^2}\,,\ \omega = \sqrt{\frac{k}{m}}. \tag{11}$$

Parameters will further be assumed to be positive. Moreover, ε [m^{-2}] will be termed the energy regulation parameter and δ [m] the amplitude parameter. Note also that its linearized solution (5) becomes time dependent as $x(t) = \alpha + A\,\cos(\omega\,t)$, $\dot{x}(t) = -\omega\,A\,\sin(\omega\,t)$.

The hopping model is now obtained by discretization of (10). Thus, the hopping dynamics are split into two phases, a flight phase ($x < 0$), where gravity alone acts upon the system's mass, and a stance phase ($x \geq 0$), where the previous dynamics are considered. In this way, the hopping model may be written as

$$\begin{cases} \ddot{x} + \omega\,\varepsilon\left(\frac{x^4}{\delta^2} - x^2\right)\dot{x} + \omega^2\,(x-\alpha) = 0 & ,\ x \geq 0 \\ \ddot{x} - \omega^2\,\alpha = 0 & ,\ x < 0 \end{cases} \tag{12}$$

with $\delta > \alpha$. As shown in Corollary 3, this system does have at least one limit cycle which is stable. In Fig. 4, the state-space solutions are illustrated and compared with the previous linearization (5). From inspection, it is remarkable to notice that the linearized model provides a close approximation to the solution of the hopping model. Particularly, regarding the maximum compression and impact speeds (the speed at the flight-stance transition). Further numerical comparisons are held until a more appropriate stage. Moreover, the linear approximation yields a good estimate for the existence of transitions between flight and stance. That is, if $\alpha - A > 0$ the phase paths of the linearized solution never intersect the $\dot{x}$ axis, and the hopping model will sustain oscillations which wont transfer to flight, by approximation. Conversely, if $\alpha - A < 0$, the hopping model will exhibit flight.

V. RUNNING MODEL

The running model is now defined, by allowing the previous hopping model to move in a two dimensional space. To do so, consider the force applied to a mass particle which is allowed to move in such space, to write $m\,\ddot{\boldsymbol{p}} = \boldsymbol{f} - m\,\mathbf{g}$. Here, $\boldsymbol{p}$ is the position of the mass and $\mathbf{g}$ the acceleration due to gravity, $\mathbf{g} = -\mathrm{g}\,\boldsymbol{y}_o$, which is fixed with respect to the inertial frame, $<\boldsymbol{x}_o\,\boldsymbol{y}_o>$.

To describe the applied forces, it is now necessary to define the state changes that occur in the flight-stance transitions. That said, as illustrated in Fig. 5(a), let the point mass be imbued with a massless leg of length ℓ_o during flight. Then, given a leg orientation during flight of $\boldsymbol{\mathcal{O}}$, a potential contact point with the ground is $\boldsymbol{p}_{\chi,\mathrm{flight}} = \boldsymbol{p} + \ell_o\,\boldsymbol{\mathcal{O}}/\,\|\boldsymbol{\mathcal{O}}\|$, where

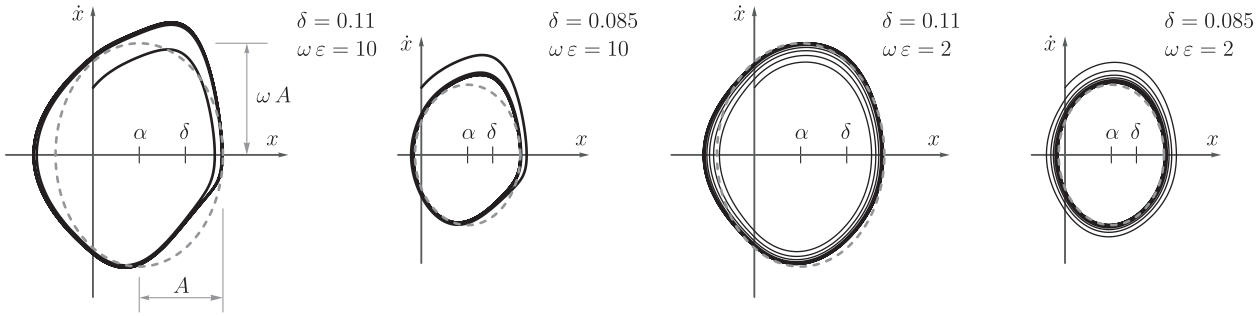

Fig. 4. Numerical solutions for the hop-in-place model (12), with $\omega = 13.34\,\mathrm{s}^{-1}$, $\alpha = \mathrm{g}/\omega^2 \approx 0.055\,\mathrm{m}$.

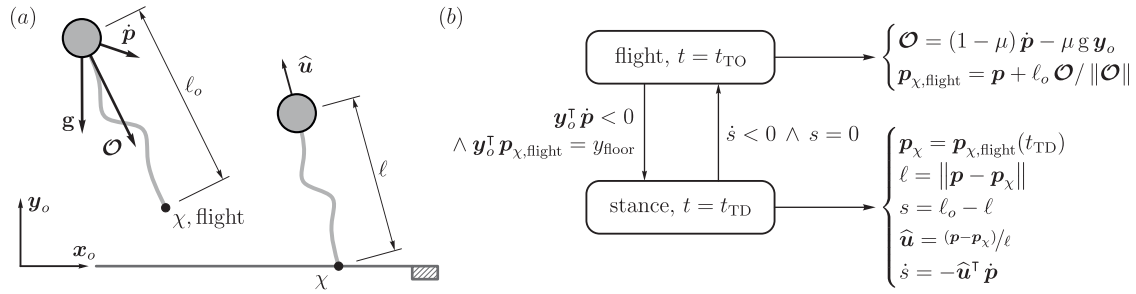

Fig. 5. Running model's illustration. (a) Flight and stance states, with main kinematic measurements. (b) State-machine and calculations summary.

the leg orientation is determined according to the VBLA model [14], as

$$\mathcal{O} = (1-\mu)\,\dot{\boldsymbol{p}} - \mu\,\mathrm{g}\,\boldsymbol{y}_o\,. \tag{13}$$

At some instant of time, $t = t_{\mathrm{TD}}$, the vertical position of this potential contact point will cross the ground, $\boldsymbol{y}_o^\intercal\,\boldsymbol{p}_{\chi,\mathrm{flight}} = y_{\mathrm{floor}}$ and $\boldsymbol{y}_o^\intercal\,\dot{\boldsymbol{p}} < 0$, which settles the contact point as $\boldsymbol{p}_\chi = \boldsymbol{p}_{\chi,\mathrm{flight}}(t_{\mathrm{TD}})$. This allows to measure leg compression as $s = \ell_o - \ell$, where $\ell = \|\boldsymbol{p} - \boldsymbol{p}_\chi\|$. Also, the leg direction is defined as $\widehat{\boldsymbol{u}} = (\boldsymbol{p} - \boldsymbol{p}_\chi)/\ell$, and the compression velocity may be obtained from projection of the point mass' velocity, $\dot{s} = -\widehat{\boldsymbol{u}}^\intercal\,\dot{\boldsymbol{p}}$. Finally, to complete the state changes, flight occurrence is defined at some time, $t = t_{\mathrm{TO}}$, where $s = 0$ and $\dot{s} < 0$. Finally, modeling the leg's support force according to the previous hopping model (12), the running model becomes

$$m\,\ddot{\boldsymbol{p}} = \begin{cases} \boldsymbol{f} - m\,\mathbf{g} & ,\ \text{stance} \\ -m\,\mathbf{g} & ,\ \text{flight} \end{cases} \tag{14}$$

$$\boldsymbol{f} = \left[m\,\omega\,\varepsilon \left(\frac{s^4}{\delta^2} - s^2 \right) \dot{s} + m\,\omega^2\,s \right] \widehat{\boldsymbol{u}}\,,\ \delta \gtrsim \sqrt{\frac{21}{10}}\,\frac{\mathrm{g}}{\omega^2} \tag{15}$$

The definition of the stance and flight states are best summarized by means of Fig. 5(b). Here, $\delta \gtrsim \sqrt{21/10}\,\mathrm{g}/\omega^2$ is a well informed estimate, that follows from the linearized solution, implying the existence of flight events ($\alpha < A$).

Proving the existence of limit cycles for this system does not seem to be a straightforward task, and this is not performed here. Nevertheless, it is appropriate to define some metrics to discuss its stability. Furthermore, since the horizontal displacement will be monotonically increasing, due to the desired locomotion, some care must be taken here in the definition of the system's state-space. That said, let the dynamics of (14) be $\dot{\boldsymbol{X}} = \boldsymbol{\phi}(\boldsymbol{X})$, where $\boldsymbol{X} = (x,\, \dot{x},\, y,\, \dot{y})$ are its state-space coordinates. Moreover, let $x(t) = \boldsymbol{x}_o^\intercal\,(\boldsymbol{p}(t) - \boldsymbol{p}(t_{\mathrm{TD}}))$, $\dot{x}(t) = \boldsymbol{x}_o^\intercal\,\dot{\boldsymbol{p}}(t)$, $y(t) = \boldsymbol{y}_o^\intercal\,(\boldsymbol{p}(t) - \boldsymbol{p}(t_{\mathrm{TD}}))$ and $\dot{y}(t) = \boldsymbol{y}_o^\intercal\,\dot{\boldsymbol{p}}(t)$. Here, $\boldsymbol{p}$ is offsetted by the the position at the instant of touchdown, $\boldsymbol{p}(t_{\mathrm{TD}})$. Note that this is a jump map which does not change the dynamics of the system. Then, let $\Sigma = \left\{ \boldsymbol{X} \in \mathbb{R}^4 \,:\, \dot{y} = 0 \,\wedge\, y > 0 \right\}$ be a Poincaré section of the state-space [12], representing the apex point of the running motion. In which case, the trajectories (solutions) will intersect Σ at some point $\boldsymbol{X}_k \in \Sigma$, at some instant of time $t = t_k$. Moreover, $T_k = t_k - t_{k-1}$ denotes elapsed time between intersections. Finally, if a fixed point is reached, such that $\boldsymbol{X}^* = \boldsymbol{X}_{k-1} = \boldsymbol{X}_k$, then it is possible to conclude that the solution is a periodic orbit (limit cycle), with period T^*. The fixed point will be

TABLE I

STABILITY ANALYSIS OF THE QUARTIC RUNNING MODEL (14), PARAMETERIZED BY $m = 50\,\mathrm{kg}$, $\ell_o = 1\,\mathrm{m}$, $\mu = 0.5$, $\delta = 0.1\,\mathrm{m}$, $\alpha = 0.03\,\mathrm{m}$, AND INITIAL CONDITIONS $\boldsymbol{X}(0) = (0\ 2.5\ 0\ -4.46)^\intercal$. RESULTS OBTAINED IN SIMULINK, USING ODE45, WITH A MAXIMUM STEP SIZE OF 10^{-3}.

$\varepsilon\,[\mathrm{m}^{-2}]$	$x^*\,[\mathrm{m}]$	$\dot{x}^*\,[\mathrm{m/s}]$	$y^*\,[\mathrm{m}]$	$T^*\,[\mathrm{ms}]$	error $< 10^{-4}$
1	0.960	2.662	0.185	563	$k = 403$
5	0.956	2.657	0.184	561	$k = 114$
10	0.955	2.655	0.183	561	$k = 54$
15	0.956	2.657	0.183	561	$k = 68$
20	0.957	2.660	0.183	561	$k = 67$
25	0.958	2.663	0.183	561	$k = 66$

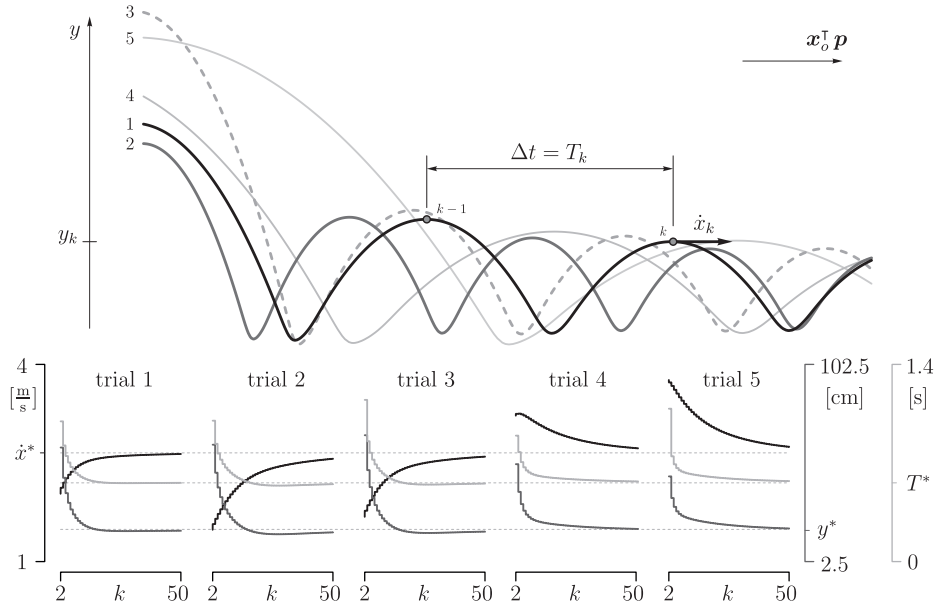

Fig. 6. Asymptotic stability of the quartic running model (14), parameterized by $m = 50\,\mathrm{kg}$, $\ell_o = 1\,\mathrm{m}$, $\mu = 0.5$, $\delta = 0.1\,\mathrm{m}$, $\alpha = 0.03\,\mathrm{m}$, $\varepsilon = 5\,\mathrm{m}^{-2}$. The attained fixed point is found to be $x^* = 0.956\,\mathrm{m}$, $\dot{x}^* = 2.657\,\mathrm{m/s}$, $y^* = 0.184\,\mathrm{m}$ and $\dot{y}^* = 0$, with period $T^* = 561\,\mathrm{ms}$.

$\boldsymbol{X}^* = (x^*, \dot{x}^*, y^*, 0)$, where $\dot{y}_k = \dot{y}^* = 0$ by virtue of the cross-section's definition.

The existence of periodic solutions is shown through simulation. In Fig. 6, five solutions are illustrated, with different initial conditions, which can be seen to converge to a fixed point, given the chosen parameterization. Solutions with backward velocity were excluded for the sake of representation. In Tab. I additional results are presented, where the changes in the fixed point can be inspected as a function of ε. Here, the number of cycles necessary for convergence are gathered, using a length measurement between successive returns, error $= \|\boldsymbol{X}_k - \boldsymbol{X}_{k-1}\|$. The fastest convergence is here observed at $\varepsilon = 10\,\mathrm{m}^{-2}$. Arguably (depending on the application's precision), the fixed point remains mostly unchanged across the present experiments. Nevertheless, the forward velocity, $\dot{x}^*$, is seen to increase for $\varepsilon > 0$, which may explain the slower convergence for large values of the energy regulation parameter. Indeed, energy regulation is synchronized with leg compression, according to the quartic oscillator's definition (2). Any synchronization with the horizontal breaking and acceleration periods occurs only by virtue of the stance symmetry, and therefore only by approximation.

A. Running model parameterization

The goal of this section is to obtain an estimate for the previous quartic running model (§V), such that it emulates the characteristics of some running gait. The approximation of the accelerated quartic model (3) will be used for this purpose. This choice is due to fact that its linear approximation yields a good estimate of the quartic hopping model (10). Nevertheless, the task of converting this one dimensional model into a two dimensional model, for the purposes of parameter estimation, necessitates the inclusion of the forward progression velocity. This task can be performed through combination of Alexander's and McMahon-Cheng's models, as illustrated in Fig. 7. A good approximation for the elastic force is given by [17] as the time dependent force

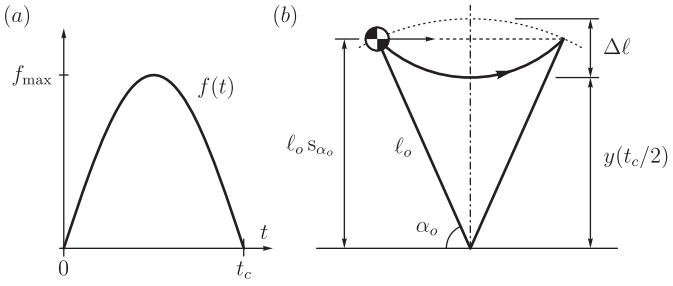

Fig. 7. (a) Sine wave approximation for the leg's force [15]. (b) Simplified model for the mass center's trajectory, redrawn from [16].

$$f(t) = f_{\max} \sin\left(\frac{\pi}{t_c}\, t\right) , \tag{16}$$

where $f_{\max}$ denotes the maximum force and t_c the contact time, as illustrated in Fig. 7(a). Following [18], this maximum force can be determined as a function of the contact time and flight time, t_f, to write

$$f_{\max} = \frac{m\,\mathrm{g}\,\pi}{4}\,\frac{1}{\mathrm{DF}} \quad , \quad \text{with} \quad \mathrm{DF} = \frac{t_c}{2\,(t_c + t_f)} , \tag{17}$$

where DF denotes the duty factor. Thus, given the maximum force, and assuming a linear elasticity for the leg, the leg stiffness follows from

$$k_p = \frac{f_{\max}}{\Delta\ell} , \quad \omega = \sqrt{\frac{k_p}{m}} , \tag{18}$$

where $\Delta\ell$ denotes the maximum leg compression. An approximate model for this displacement is given in [16]. As

illustrated in Fig. 7(b), this maximum displacement can be computed as $\Delta\ell = \ell_o - y\,(t_c/2)$, where $y\,(t_c/2)$ denotes the vertical displacement at midstance. This displacement may be estimated with recourse to (16) by expressing the vertical acceleration, $\ddot{y}(t) = f(t)/m - \mathrm{g}$, which can be integrated to yield

$$\Delta\ell = \ell_o - \ell_o \,\sin\,\alpha_o + \frac{f_{\max}}{m}\left(\frac{t_c}{\pi}\right)^2 - \frac{\mathrm{g}}{8}\,t_c^2\,, \tag{19}$$

$$v_y(t_{\mathrm{TD}}) = \frac{\mathrm{g}\,t_c}{2} - \frac{f_{\max}\,t_c}{m\,\pi}\,. \tag{20}$$

Here, the initial impact velocity $v_y(t_{\mathrm{TD}})$ was also determined. To complete the deployment of these models, leg angle at touchdown may also be determined with recourse to Fig. 7(b), as

$$\alpha_o = \arccos\!\left(\frac{v_x\,t_c}{2\,\ell_o}\right)\,. \tag{21}$$

In the present running model, leg orientation is determined according to the VBLA model (13). As illustrated in Fig. 5(a), let the leg direction be $\alpha_o = -\arctan\,(\boldsymbol{y}_o^{\intercal}\boldsymbol{\mathcal{O}}, \boldsymbol{x}_o^{\intercal}\boldsymbol{\mathcal{O}})$. Then, the VBLA parameter can be determined through

$$\mu = \frac{v_y + v_x\,\tan(\alpha_o)}{\mathrm{g} + v_y + v_x\,\tan(\alpha_o)}\,, \tag{22}$$

where the horizontal velocity may be specified from desired value, $v_x = v_d$, while the vertical velocity may be determined from the previous estimate (20), $v_y = v_y(t_{\mathrm{TD}})$.

To conclude, consider now that the maximum compression is given by the quartic hopping model (12) and its corresponding approximation (5). Then $\Delta\ell = \alpha + A(\alpha,\delta)$, where $A(\alpha,\delta)$ was previously obtained in (9). Finally, solving for δ, yields its value, from previously determined $\Delta\ell$,

$$\delta = \frac{1}{\sqrt{2}}\sqrt{9\,\alpha^2 - 2\,\alpha\,\Delta\ell + \Delta\ell^2 - \frac{24\,\alpha^4}{5\,\alpha^2 - 2\,\alpha\,\Delta\ell + \Delta\ell^2}}\,. \tag{23}$$

B. Marathon pace

Following the previous synthesis, the quartic running model (§V) is now tuned in such a way that it mimics the external dynamics of a running gait. The input variables for design and the resulting parameters are summarized in Tab. II, following the parameterization described in §V-A. The resulting limit cycle solution is illustrated in Fig. 8, which is now compared to the input values and also the estimated characteristics of the running gait. The results are best summarized through Tab. III, to say that the proposed parameterization yields a remarkable approximation of the desired gait. This degree of approximation is reliant on the fact that maximum compression is well estimated through the quartic model's linearization (§III), with an error of $0.2\,\mathrm{mm}$. Consequently, maximum force is also well estimated when the energy regulation is low ($\varepsilon = 5\,\mathrm{m}^{-2}$), since the dominant term is elastic. The horizontal velocity's approximation is not as strong, which in turn yields an opportunity to discuss the possibility of velocity regulation. In this regard, the amplitude parameter, δ, may be chosen as a way to increase the separation velocity at takeoff, which will in turn increase the horizontal velocity. A value of $\delta = 0.1247\,\mathrm{m}$ is found to converge to the desired velocity, as shown in Tab. III. Increasing the takeoff velocity will also change the vertical velocity, which will in turn change the accuracy of the characteristics related to the vertical oscillation.

TABLE II

RUNNING MODEL PARAMETERS FOR A MARATHON PACE VELOCITY, FOLLOWING QUARTIC MODEL INTERPRETATION.

Symbol	Value [units]	Nomenclature
v_d	$5.55\,[\mathrm{m/s}]$	Desired velocity [11]
m	$55.17\,[\mathrm{kg}]$	Locomotor's mass [11]
ℓ_o	$1\,[\mathrm{m}]$	Rest length
t_c	$170\,[\mathrm{ms}]$	Stance/contact time [11]
DF	0.25	Duty factor [11], (17)
$f_{\max}$	$1700\,[\mathrm{N}]$	Maximum force (17)
α_o	$61.9\,[\mathrm{deg}]$	Angle of attack (21)
$v_y(t_{\mathrm{TD}})$	$-0.834\,[\mathrm{m/s}]$	Vertical impact velocity 20)
μ	0.493	VBLA tuning parameter (22)
$\Delta\ell$	$0.173\,[\mathrm{m}]$	Maximum leg compression (19)
k_p	$9824\,[\mathrm{N/m}]$	Leg stiffness (18)
ω	$13.34\,[\mathrm{rad/s}]$	Stance frequency (18)
α	$0.0551\,[\mathrm{m}]$	Acceleration bias (11)
δ	$0.1219\,[\mathrm{m}]$	Amplitude parameter (23)

TABLE III

COMPARISON BETWEEN THE DESIRED, OR ESTIMATED VALUES, WITH THE RESULTS IN FIG. III, FOR $\varepsilon = 5\,\mathrm{m}^{-2}$.

	desired / estimated	result ($\delta = 0.1219\,\mathrm{m}$)	speed regulated ($\delta = 0.1247\,\mathrm{m}$)
$v_x\,[\mathrm{m/s}]$	5.55	5.461	5.55
$t_c\,[\mathrm{ms}]$	170	176	175
DF	0.25	0.254	0.249
$f_{\max}\,[\mathrm{N}]$	1700	1725.5	1768.5
$\alpha_o\,[\mathrm{deg}]$	61.9	62.24	61.9
$v_y\,[\mathrm{m/s}]$	-0.834	-0.835	-0.868
$\Delta\ell\,[\mathrm{cm}]$	17.3	17.28	17.68

VI. DISCUSSION

The quartic damping model introduces work loops of dissipation and energy generation, which imbue the model with limit cycle convergence. These loops can be inspected from the force-displacement profiles, in Fig. 8. The success of the model in replicating running gaits is also due to the synchronism between the compression-extension phases of the leg with the phases of horizontal breaking-acceleration. Such synchronicity does not occur in walking gaits, where multiple compression-extension phases occur during stance. Thus, it remains to be seen how the present ideas may be extended to modeling walking gaits. Nevertheless, it is well known from the phenomenology of muscle dynamics, and its application to the construction of walking models [19], that such regulation must be present during walking as well.

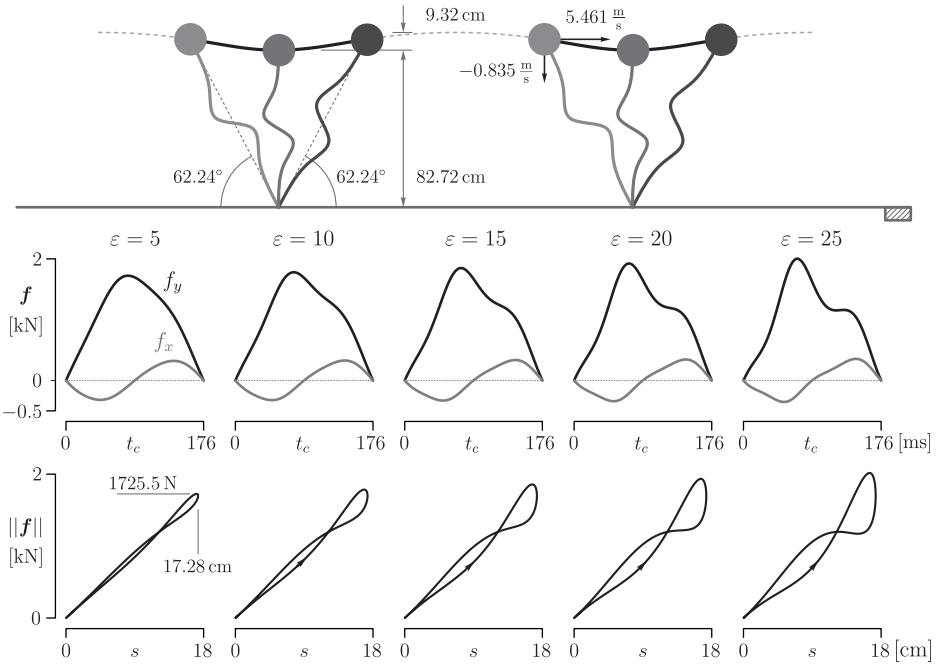

Fig. 8. Illustration of the quartic running model's (14) limit cycle trajectory, emulating the dynamics of long distance running (Tab. II), with $\varepsilon = 5\,\mathrm{m}^{-2}$. The energy regulation parameter is changed to illustrate the changes in the force pattern and the displacement-force pattern. The fixed point is $\boldsymbol{X}^* = (1.396\ 5.461\ 0.0355\ 0)^\intercal$, with $T^* = 346\,\mathrm{ms}$, resulting in a flight time of $t_f = 170\,\mathrm{ms}$, or $\mathrm{DF} = 0.254$.

As it stands, the quartic running model represents a model of impedance, for interaction with the ground. The model represents a template for locomotion which can be anchored to a rigid body model by means of force or impedance control techniques. Adding appropriate control features for the regulation of posture and the leg swing, stable locomotion of a rigid body mechanism can be achieved.

VII. CONCLUSION

The present quartic model was able to replicate the gait characteristics of running at a marathon pace. Approximations of the model, together with known stance models, allowed to provide a model for its parameterization.

APPENDIX

This section deals with the dynamics of Liénard systems [12]. That is, systems of the form

$$\ddot{x} + h(x)\,\dot{x} + g(x) = 0\,. \tag{24}$$

Analysis of these nonlinear systems is conveniently performed in a space of coordinates referred to as the Liénard plane [20], described by

$$\dot{x} = y - H(x)\,, \quad \dot{y} = -g(x)\,, \text{ with } H(x) = \int_0^x h(u)\,du\,. \tag{25}$$

For the ensuing theorems, it is also useful to define $G(x) = \int_0^x g(u)\,du$. That said, to show the existence of limit cycles consider the following theorem [12], [21].

Theorem 1 (Liénard): The system (25) has a unique limit cycle and the limit cycle is asymptotically stable, if the following conditions hold true.

1) $h(x)$ is even and continuous in $\left]-\infty, +\infty\right[$;
2) $H(x)$ has a unique positive zero $a > 0$, and $H(x)\ (x-a) > 0$ for $x > 0$, $x \neq a$;
3) $H(x)$ is monotone increasing in $\left]a, +\infty\right[$, and $H(x) \to +\infty$ as $x \to +\infty$;
4) $g(x)$ is odd and continuous in $\left]-\infty, +\infty\right[$, and $x\,g(x) > 0$, $\forall\, x \neq 0$.

The following theorem establishes an upper bound for the limit cycle's trajectory [21].

Theorem 2 (Lijun-Xianwu): In addition to the conditions of Theorem 1, and further assuming that

1) $h(x)$ has a unique positive zero $b > 0$ and $h(x)\ (x-b) > 0$ for $x > 0$, $x \neq b$;
2) $h(x)\,/g(x)$ is monotone increasing on $\left]b, +\infty\right[$;
3) $\int_0^{x^*} H(s)\,g(s)\,ds > 0$ for sufficiently large $x^* > 0$,

then the unique limit cycle in Theorem 1 is located in the strip region $\left|x\right| < x^*$.

Corollary 1 (Quartic oscillator): The system (2), with $\varepsilon > 0$ and $\delta > 0$, has a unique and stable limit cycle. Its state-space trajectory, $\Gamma(x, \dot{x})$, is contained in $\Gamma \in \left\{(x, \dot{x}) \in \mathbb{R}^2 \,:\, x^2 + \dot{x}^2 > \delta^2 \,\vee\, |x| < \sqrt{\tfrac{7}{3}}\,\delta\right\}$.

Proof: The functions $h(x)$ and $g(x)$ satisfy the symmetry and sign conditions required by Thm. 1. The primitive $H(x)$ has a unique positive zero at $a = \sqrt{5/3}\,\delta$, and $H(x)$ is mon. inc. for $x > \delta$. Thus the system admits a unique, asymptotically stable limit cycle. Moreover, $h(x)$ has a unique positive zero at $b = \delta$ and satisfies the necessary sign condition of Thm. 2. Also, the ratio $h(x)/g(x)$ is strictly increasing for $x > \delta$, and the integral condition (3) is met,

with the transition to positivity at $x^* = \sqrt{7/3}\,\delta$. Finally, the inner bound can be found via Lyapunov analysis. Using $\mathcal{V}(\boldsymbol{z}) = \frac{1}{2}(x^2 + v^2)$ and its gradient. It can be found that the equilibrium is unstable and that all trajectories starting in $0 < x^2 + \dot{x}^2 < \delta^2$ are bound to escape this region. ■

Theorem 3 (Dragilëv): Let the following conditions hold:

1) $x\,g(x) > 0$ when $x \neq 0$, and $G(\pm\infty) = +\infty$;
2) $x\,H(x) < 0$ when $x \neq 0$ and $|x|$ is sufficiently small;
3) There exist constants $M > 0$ and $K > K'$ such that

$$H(x) \geq K \;\forall\; x > M \quad \text{and} \quad H(x) \leq K' \;\forall\; x < -M\,.$$

Then system (25) has stable limit cycles.

Corollary 2 (Accelerated quartic oscillator): The system (3), with $\varepsilon > 0$ and $\delta > \alpha > 0$, has at least one limit cycle which is stable.

Proof: To verify the conditions of Thm. 3, the coordinates of (3) need to be translated by $\xi = x - \alpha$, to write $\ddot{\xi} + h(\xi)\,\dot{\xi} + g(\xi) = 0$. In which case, cond. (1) is straightforward to verify. To satisfy cond. (2), the slope of H must be negative in the origin, $h(0) < 0$, which is verified if $\delta > \alpha$. Cond. (3) holds, since $H(\xi) \sim \xi^5$ for large ξ. ■

The following theorem establishes the existence of limit cycles in Liénard systems which lack symmetry [22].

Theorem 4 (Cioni-Villari): The system (25) has at least one periodic solution if the following conditions hold true.

1) $h, g : \mathbb{R} \to \mathbb{R}$ are continuous and $g(x)$ is locally Lipschitz. Also $x\,g(x) > 0 \,\forall\, x \neq 0$;
2) $g(x)\,H(x) < 0$ for $|x| < \epsilon$ and $x \neq 0$, where ϵ is arbitrarily small;
3) Exist $K_1, K_2 \in \mathbb{R}$, $K_1 > K_2$ such that

$$\begin{aligned} H(x) &\geq K_1, \quad x > c_1 > 0 \\ H(x) &\leq K_2, \quad x < c_2 < 0; \end{aligned}$$

4) $\limsup_{x\to\pm\infty} G(x) \pm H(x) = +\infty$.

Corollary 3 (Hopping model): The system (12), with $\varepsilon > 0$ and $\delta > \alpha > 0$, has at least one limit cycle which is stable.

Proof: After coordinate transformation, $\xi = x - \alpha$, cond. (1) of Thm. 4 is straightforward to verify. Now, noting that $H(\xi) = \overline{H}(\xi) - \overline{H}(0)$ for $\xi \geq -\alpha$ and $H(\xi) = -\overline{H}(0)$ for $\xi < -\alpha$, cond. (2) can be verified when $-\overline{H}(0) > 0$, which holds for $\delta > \sqrt{3/5}\,\alpha$, together with the imposition that the slope of H is negative at the origin, $h(0) < 0$, which occurs when $\delta > \alpha > \sqrt{3/5}\,\alpha$. Cond. (3) is verified by first noting that K_1 may be arbitrarily large, since H is strictly monotone increasing. Also, since H is bound by $-\overline{H}(0)$, for $\xi < 0$, there must exist such $K_1 > K_2$ relation. Finally, cond. (4) is ensured by the monotonicity of the functions. ■

ACKNOWLEDGMENT

The authors acknowledge Fundação para a Ciência e a Tecnologia (FCT) for its financial support via LAETA (project https://doi.org/10.54499/UID/50022/2025). This work was supported by FCT - Fundação para a Ciência e a Tecnologia, under the PhD grant SFRH/BD/137986/2018.

REFERENCES

[1] H. Geyer, A. Seyfarth, and R. Blickhan, "Compliant leg behaviour explains basic dynamics of walking and running," *Proceedings of the Royal Society B: Biological Sciences*, vol. 273, no. 1603, pp. 2861–2867, 2006.

[2] A. S. Carvalho and J. M. Martins, "Bipedal running through imposition of a stabilizing contact force," in *2018 IEEE International Conference on Autonomous Robot Systems and Competitions (ICARSC)*. IEEE, 2018, pp. 42–47.

[3] A. Albu-Schäffer, C. Ott, U. Frese, and G. Hirzinger, "Cartesian impedance control of redundant robots: recent results with the dlr-light-weight-arms," *2003 IEEE International Conference on Robotics and Automation*, vol. 3, pp. 3704–3709, 2003.

[4] D. Lakatos, W. Friedl, and A. Albu-Schäffer, "Eigenmodes of non-linear dynamics: Definition, existence, and embodiment into legged robots with elastic elements," *IEEE Robotics and Automation Letters*, vol. 2, no. 2, pp. 1062–1069, 2017.

[5] H. Shinkawa, T. Kawase, T. Miyazaki, T. Kanno, M. Sogabe, and K. Kawashima, "Limit cycle generation with pneumatically driven physical reservoir computing," in *2023 IEEE International Conference on Robotics and Automation (ICRA)*. IEEE, 2023, pp. 537–543.

[6] F. Li, L. Pang, and T. Dai, "Cpg motion controller based on van der pol nonlinear oscillator for a quadruped robot," in *2023 5th International Conference on Robotics, Intelligent Control and Artificial Intelligence (RICAI)*. IEEE, 2023, pp. 236–239.

[7] I. U. Cayetano-Jimenez, D. Arriaga-Ventura, E. A. Martinez-Ríos, and R. Bustamante-Bello, "Van der pol oscillators and phase-locked loops: A transparent model for central pattern generators in bioinspired robotics," *IEEE Access*, 2024.

[8] E. Burdet, D. W. Franklin, and T. E. Milner, *Human robotics: neuromechanics and motor control*. MIT press, 2013.

[9] H. Geyer, A. Seyfarth, and R. Blickhan, "Positive force feedback in bouncing gaits?" *Proceedings of the Royal Society of London. Series B: Biological Sciences*, vol. 270, no. 1529, pp. 2173–2183, 2003.

[10] M. A. Sharbafi and A. Seyfarth, "Model zoo: Extended conceptual models," *Bioinspired Legged Locomotion: Models, Concepts, Control and Applications*, p. 109, 2017.

[11] J. Santos-Concejero, N. Tam, D. Coetzee, J. Oliván, T. Noakes, and R. Tucker, "Are gait characteristics and ground reaction forces related to energy cost of running in elite kenyan runners?" *Journal of sports sciences*, vol. 35, no. 6, pp. 531–538, 2017.

[12] D. Jordan and P. Smith, *Nonlinear ordinary differential equations: an introduction for scientists and engineers*. OUP Oxford, 2007.

[13] R. Goebel, R. G. Sanfelice, and A. R. Teel, "Hybrid dynamical systems," *IEEE control systems magazine*, vol. 29, no. 2, pp. 28–93, 2009.

[14] M. A. Sharbafi and A. Seyfarth, "Vbla, a swing leg control approach for humans and robots," in *2016 IEEE-RAS 16th International Conference on Humanoid Robots (Humanoids)*. IEEE, 2016, pp. 952–957.

[15] R. M. Alexander, *Principles of animal locomotion*. Princeton university press, 2003.

[16] T. A. McMahon and G. C. Cheng, "The mechanics of running: how does stiffness couple with speed?" *Journal of biomechanics*, vol. 23, pp. 65–78, 1990.

[17] R. M. Alexander, "On the synchronization of breathing with running in wallabies (macropus spp.) and horses (equus caballus)," *Journal of Zoology*, vol. 218, no. 1, pp. 69–85, 1989.

[18] G. Dalleau, A. Belli, F. Viale, J.-R. Lacour, and M. Bourdin, "A simple method for field measurements of leg stiffness in hopping," *International journal of sports medicine*, vol. 25, no. 03, pp. 170–176, 2004.

[19] S. Song and H. Geyer, "Generalization of a muscle-reflex control model to 3d walking," in *2013 35th Annual International Conference of the IEEE Engineering in Medicine and Biology Society (EMBC)*. IEEE, 2013, pp. 7463–7466.

[20] Y. Ye and S.-l. Cai, *Theory of limit cycles*. American Mathematical Soc., 1986, vol. 66.

[21] Y. Lijun and Z. Xianwu, "An upper bound for the amplitude of limit cycles in liénard systems with symmetry," *Journal of Differential Equations*, vol. 258, no. 8, pp. 2701–2710, 2015.

[22] M. Cioni and G. Villari, "An extension of dragilev's theorem for the existence of periodic solutions of the liénard equation," *Nonlinear Analysis: Theory, Methods & Applications*, vol. 127, pp. 55–70, 2015.